Photonics and Nanostructures - Fundamentals and Applications xxx (xxxx) xxx–xxx

Contents lists available at ScienceDirect

Photonics and Nanostructures - Fundamentals and Applications

journal homepage: www.elsevier.com/locate/photonics

Invited Paper

Optical coupling characteristics between a circular defect resonator and a waveguide in a two-dimensional photonic crystal slab

Yuji Miyamoto, Yifan Xiong, Tomoyuki Okada, Masato Morifuji*, Hirotake Kajii, Masahiko Kondow

Department of Electronic Engineering, Graduate School of Engineering, Osaka University, 2-1 Yamada-oka, Suita, Osaka 565-0871, Japan

ARTICLE INFO

PACS:
42.55.Tv
42.60.Da

Keywords:
Wavelength division multiplexing
Photonic crystal

ABSTRACT

To develop a wavelength division multiplexing (WDM) device using a photonic crystal (PC), we investigate coupling strength between a circular cavity resonator and a waveguide with various structural parameters. In the WDM device, light signals with various wavelengths generated in different cavity resonators travel through a single waveguide. Careful tuning of the cavity-waveguide coupling is necessary for practical operations, since the light signals must have the same intensities in the waveguide. Carrying out three-dimensional finite-differential time-domain (FDTD) calculations along with photonic bands, we search for the optimum structure for the WDM.

1. Introduction

The huge power consumption induced by the rapid increase of data in the IP traffic will be a crucial problem shortly [1]. A new device that has low power consumption, high operation speed, and integrability, is strongly demanded. The photonic crystal (PC) in a two-dimensional slab is attracting great attention for such novel optical devices. Then, we focus on a wavelength division multiplexing (WDM) device, in which light signals with various wavelengths travel through a single waveguide [2,3]. For the WDM device, first, we have to develop a high-performance cavity resonator as a laser light source. We have proposed a laser structure as shown in Fig. 1(a) and (b), where the current is vertically injected into a circular cavity resonator. Compared with a laser structure in which current is horizontally injected into a linear cavity resonator [4], the present structure is advantageous for integrability because of smaller footprint [5,6]. Also, owing to a large cross-section of the current injection area, this laser has a low resistance which is necessary for the low power consumption and high-speed operation. Furthermore, according to our preliminary study, the circular defect laser operates at the speed of 50 Gbps [7]. Therefore, this structure satisfies all the requirements for the WDM device.

For practical operations of the WDM device, light intensities arising in the different cavities must have the same magnitude. However, coupling strength to a waveguide depends on frequency. Thus, the next step for development of the WDM device is to adjust the cavity-waveguide coupling.

In this paper, we theoretically investigate the coupling strength between the circular cavity and the waveguide. Although we have studied the cavity-waveguide coupling [8,9], we neglected the thickness of the device. Carrying out calculations for a realistic device structure which has a finite thickness, we evaluate the coupling efficiencies under various structural parameters.

2. Device structure

Fig. 1(a) and (b) shows the device structure we investigate in this study. We note that a GaAs cap layer is not shown for visibility. As shown in Fig. 1(a), there are a circular defect and a waveguide set in a triangular array of air holes. From the requirement that the device operates in the 1.3 μm wavelength range, we set the lattice constant a of the photonic crystal to 340 nm, and the radius of the air holes r to 0.3 a. The waveguide is constructed by linearly removing air holes. This structure is built in a semiconductor slab where a GaAs core layer is cladded by AlO_x layers. We can realize this structure by oxidizing AlGaAs layers of an AlGaAs/GaAs/AlGaAs heterostructure after fabrication of air holes. Since the AlGaAs is covered with the GaAs cap layer, the oxidation occurs around the air holes. Thus, the AlGaAs regions just at the cavity remain unoxidized. The remaining AlGaAs regions act as funnels for carrier injection. Therefore, we expect that light confinement due to AlO_x region and current injection due to the funnels are compatible. We set the thickness of the GaAs core layer and that of the AlO_x cladding layer to 320 nm and 550 nm, respectively. We

* Corresponding author.
E-mail address: morifuji@eei.eng.osaka-u.ac.jp (M. Morifuji).

https://doi.org/10.1016/j.photonics.2018.06.002
Received 12 October 2017; Received in revised form 5 June 2018; Accepted 5 June 2018

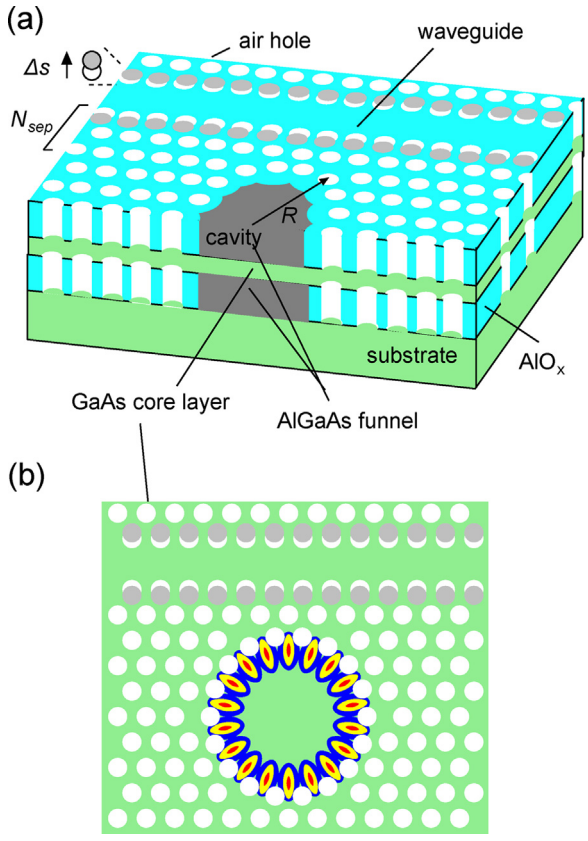

Fig. 1. (a) Schematic structure of the device studied in this paper. In the array of air holes, there is a circular cavity (radius R) and a waveguide separated by N_{sep} rows of air holes. Displacement of air holes on the sides of the waveguide is denoted as Δs where $\Delta s > 0$ means widening the waveguide. (b) Slice cut of the GaAs core layer where whispering gallery mode in the circular cavity is also shown.

constructed a circular defect resonator by removing hexagonally aligned 19 air holes and modified positions of air holes on the periphery so that they align with a circle.

Although many cavity modes can arise in the circular cavity, most of them have small Q, and thus they are irrelevant to the laser operation, since light confinement of this AlO_x clad is not so strong. Only the whispering gallery mode (WGM) shown in Fig. 1(b) which has an exceptionally large Q [10,11] is relevant to the laser operation. The Q factor of the WGM is as high as 10,000, which is high enough for the laser operation.

We pay attention to several structural parameters that determine the cavity-waveguide coupling characteristics. The number of rows of air holes between the cavity and the waveguide N_{sep} strongly affects on the coupling strength. By changing the radius of the circular defect R (defined as the length from the center of the defect to the center of the surrounding air holes), we can vary the wavelength of the output light. We also vary the waveguide mode by changing the width of the waveguide. We shifted the air holes on both sides of the waveguide by Δs as shown in Fig. 1(a), where the gray circles are the shifted ones.

3. Calculations

3.1. FDTD calculations

We carried out FDTD calculations for the PC structure shown in Fig. 1 using a self-made fortran program validated by reproducing some typical PC cavities such as L3, H2 *etc*. First, we calculated temporal evolution of the electric and magnetic fields $\boldsymbol{E}$ and $\boldsymbol{H}$ by numerically solving the Maxwell's equations

$$\frac{\partial \boldsymbol{E}(\boldsymbol{r}, t)}{\partial t} = \frac{1}{\epsilon(\boldsymbol{r})\epsilon_0}\mathrm{rot}\,\boldsymbol{H}(\boldsymbol{r}, t) \tag{1}$$

and

$$\frac{\partial \boldsymbol{H}(\boldsymbol{r}, t)}{\partial t} = -\frac{1}{\mu_0}\mathrm{rot}\,\boldsymbol{E}(\boldsymbol{r}, t) \tag{2}$$

in the discretized space and time. In Eq. (1), $\epsilon(\boldsymbol{r})$ is the dielectric constant of the device. We have used the values: $\epsilon_{\mathrm{GaAs}} = 11.9$, $\epsilon_{\mathrm{AlGaAs}} = 8.6$, and $\epsilon_{\mathrm{AlOx}} = 2.4$ for the constituent materials. The spatial mesh size is $\Delta x = 10$ nm, which is less than 1/10 of a typical wavelength of the magnetic fields. The time interval is $\Delta t = 1.75 \times 10^{-17}$ [s] so that stability of the simulation is warranted. We used Mur's second formula at the outer boundary of the calculation region so that the reflection at the boundary does not occur.

Next, from the electromagnetic fields, we calculated a temporal Fourier transformation of the magnetic field at a suitable position $\boldsymbol{r}_0$ in the cavity as

$$S(\omega, \boldsymbol{r}_0) = \int_0^T e^{i\omega t} H_z(\boldsymbol{r}_0, t)\,\mathrm{d}t. \tag{3}$$

Generally, $S(\omega, \boldsymbol{r}_0)$ vanishes for large T because of destructive interference due to random phase. However, only when ω coincides a frequency of a cavity mode ω_c and the cavity mode has a finite amplitude at $\boldsymbol{r}_0$, $S(\omega, \boldsymbol{r}_0)$ takes a large value since constructive interference occurs. In Fig. 2, we plot the cavity mode frequency ω_c as a function of the cavity radius R evaluated from the spectrum intensity, $|S(\omega, \boldsymbol{r}_0)|^2$ whose peak corresponds to ω_c. Fig. 2 indicates that ω_c becomes smaller as R becomes larger. This is because that the WGM is formed along the circumference of the resonator and its wavelength is proportional to the length of the circumference [12,13]. This figure also shows that cavity radius variation of 6.4 nm corresponds to a wavelength variation of 10 nm.

Then, from the results of the FDTD calculations, we also calculated the Q factor from the electromagnetic energy

$$U(t) = \frac{1}{2}\int d\boldsymbol{r}^3[\epsilon(\boldsymbol{r})\epsilon_0|\boldsymbol{E}(\boldsymbol{r}, t)|^2 + \mu_0|\boldsymbol{H}(\boldsymbol{r}, t)|^2] \tag{4}$$

and the definition of the Q factor

$$U(t) \propto \exp\left(\frac{-\omega_c t}{Q}\right). \tag{5}$$

We investigated the cavity-waveguide coupling as follows: Let Q_0 be the

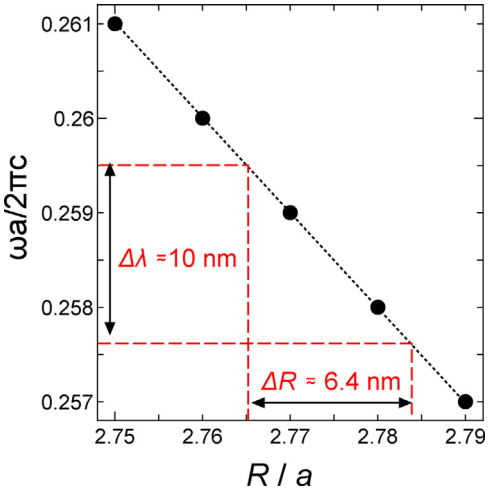

Fig. 2. Resonant frequency of the whispering gallery mode as a function of cavity radius. Dashed lines show that 6.4 nm of cavity radius difference yields 10 nm difference in output wavelength.